International Communications in Heat and Mass Transfer 60 (2015) 21–31

Contents lists available at ScienceDirect

International Communications in Heat and Mass Transfer

journal homepage: www.elsevier.com/locate/ichmt

Convective heat transfer and second law analysis of non-Newtonian fluid flows with variable thermophysical properties in circular channels☆

Mostafa Shojaeian, Mehmet Yildiz, Ali Koşar *

Mechatronics Engineering Program, Faculty of Engineering and Natural Sciences, Sabanci University, Tuzla, Istanbul 34956, Turkey

ARTICLE INFO

Available online 10 December 2014

Keywords:
Thermophysical properties
Non-Newtonian flow
Nusselt number
Viscous heating

ABSTRACT

This study presents an analytical solution, for fully developed non-Newtonian fluid flows in circular channels under isoflux thermal boundary conditions based on perturbation techniques. Since the physical properties are generally a function of temperature and may not be assumed constant under certain circumstances, the change in viscosity and thermal conductivity with temperature was taken into account. Viscous dissipation term was also included in the performed analysis. In this study, first closed form expressions for velocity, temperature distributions, and Nusselt numbers corresponding to constant thermophysical properties were given in terms of governing parameters. Then, numerical calculation was performed to obtain the values of Nusselt number and global entropy generation for variable thermophysical properties. The results revealed that neglecting the property variation significantly affects heat transfer characteristics and entropy generation, in which the deviation from the constant physical property assumption may reach up to about 32.6%.

1. Introduction

Being interdisciplinary and having a wide range of application in industry, non-Newtonian fluid flows require a thorough study in terms of experimental, numerical and analytical aspects to find applications in emerging fields. In contrast to Newtonian fluids, the viscosity of non-Newtonian fluids, which are typically involved in complex material structures such as foams, polymer melts, emulsions, slurries, and solutions, shows a different trend when exposed to variations in shear rate. Therefore, an appropriate viscosity model should be implemented for their analysis. Non-Newtonian fluids offer an attractive subject for scientists and engineers from different disciplines to explore mathematical models for relating stress, deformation and heat transfer behaviors [1–4].

A large number of experimental and numerical studies regarding non-Newtonian fluids have been reported in the literature. However, few experimental studies have been conducted to investigate convective heat transfer characteristics of non-Newtonian fluids [5–10]. On the other hand, many numerical investigations on heat transfer of non-Newtonian fluids have been reported in the literature including a wide range of different cases such as forced convection [11–15], natural convection [16–19] and mixed convection [20–23] in addition to the consideration of fluids exposed to external fields such as magnetic field (known as MHD flow [24–26]) and electric field (electroosmosis [27–29]).

Many researchers concentrated on an analytical approach to examine heat and fluid flow characteristics of non-Newtonian fluids for internal convection, which is important for giving an insight into a better design for devices involving non-Newtonian fluids. As a result of such efforts, many studies are present in the literature. For example, Chiba et al. [30] analytically studied convective heat transfer in a pipe exposed to non-axisymmetric heat loads with constant properties including the viscous heating term. Their analysis of heat transfer was performed by using an integral transform technique, 'Vodicka's method', at which Brinkman number and rheological properties effects on local Nusselt number were exhibited. Pinho and Coelho [31] presented an analytical solution for thermally and hydrodynamically fully developed viscoelastic fluid flows inside a concentric annulus by simplification of the Phan-Thien–Tanner constitutive equation subject to both constant wall heat fluxes and constant wall temperatures under the consideration of viscous dissipation term. They obtained some expressions for the inner and outer Nusselt number in terms of appropriate dimensionless parameters. Manglik and Ding [32] analytically solved the fully developed laminar power-law fluid flows based on the Galerkin integral method in double-sine shaped channels for constant temperature and heat flux thermal boundary conditions and obtained results for friction factor and Nusselt number. Thayalan and Hung [33] presented a theoretical solution based on the Brinkman-extended Darcy model for power-law fluid flows in porous media. They derived an expression for the overall Nusselt number based on a proposed parabolic model and did their analysis on convective heat transfer characteristics relevant to porous

☆ Communicated by W.J. Minkowycz.

* Corresponding author.
E-mail address: kosara@sabanciuniv.edu (A. Koşar).

http://dx.doi.org/10.1016/j.icheatmasstransfer.2014.12.002
0735-1933/

Nomenclature

A	constant defined by Eqs. (22) or (23)
A'	constant defined by Eqs. (24) or (25)
b	A coefficient in Eq. (4)
Br	Brinkman number
$C_1,\ldots, C_6$	constant defined in Eq. (34)
CP	constant property
c_p	specific heat at constant pressure
D	hydraulic diameter
k	thermal conductivity of fluid
$m^{\bullet}$	mass flow rate
n	power-law index
N_s	dimensionless entropy generation number
$<N_s>$	global entropy generation rate
Nu	Nusselt number
p	pressure
Pe	Peclet number
q''	heat flux
R	dimensional radial position in coordinate system
r	dimensionless radial position in coordinate system
Re	Reynolds number
S	cross-section area
$S^{\bullet}$	entropy generation
T	temperature
U	dimensional velocity component in the X direction
u	dimensionless velocity component in the X direction
U_m	mean velocity
VP	variable property
X	dimensional axial position in the coordinate system
x	dimensionless axial position in the coordinate system

Greek symbols

Λ	perimeter
τ	shear stress
γ	specific heat ratio of fluid
μ	dynamic viscosity of fluid
ρ	density of fluid
θ	dimensionless temperature
ϕ	consistency factor
φ	source term (here, viscous dissipation)
Ω	defined as $q'' r_0/T_i k$
ε	defined by Eq. (7)
ε_k	defined by Eq. (8)
Γ	$\varepsilon_k/\varepsilon$

Subscripts

i	fluid properties at the inlet
m	mean or bulk
s	reference value
w	wall

media. Chen [34] presented an analytical solution for convective heat transfer in electroosmotic power-law fluid flows between two parallel-plates by obtaining some expressions for velocity and temperature distributions, and fully developed Nusselt number. Similar studies for a circular channel, based on the linearized Poisson–Boltzmann distribution equation, and for viscoelastic fluids related to Phan-Thien–Tanner (PTT) and Finitely-Extensible-Nonlinear-Elastic (FENE-P) models were also carried out [35,36]. Tso et al. [37] did a theoretical analysis on heat transfer of hydrodynamically and thermally fully developed laminar non-Newtonian fluids between parallel-plates while considering viscous dissipation effects for asymmetric heating and presented a Nusselt number expression in terms of Brinkman number and power-law index. Mahmud and Fraser [38] used the first and second laws of thermodynamics to derive some expressions for asymptotic Nusselt and entropy generation for flows of a power-law fluid in circular channels and between parallel-plates. In our previous work [39], convective heat transfer and entropy generation characteristics of both hydrodynamically and thermally fully developed laminar Newtonian and non-Newtonian fluid flows in parallel-plate microchannels were analytically investigated, and Nusselt number, global entropy generation, and Bejan number expressions were presented.

In all the above-mentioned studies, the constant thermophysical property assumption was used. However, this assumption may not be reasonable if there is a significant variation in thermophysical properties with temperature. To the authors' best knowledge, there are only a few studies in the literature related to convective heat transfer of non-Newtonian fluids, which consider the change in thermophysical properties as a function of temperature [40–42]. Molaei-Dehkordi and Memari [43] also carried out a numerical investigation on the transient, hydrodynamically fully developed, laminar power-law fluids flow in the thermally developing entrance region of circular tube, while taking the viscous dissipation, axial conduction, and temperature-dependent viscosity into account. To address the gap in the literature, this study presents an analytical model for convective heat transfer of power-law fluids in circular channels subjected to isoflux thermal wall boundary conditions, while accounting for the effect of viscous dissipation. The presented analysis, based on perturbation method, focuses on Nusselt number and global entropy generation in the case of the presence of thermophysical property variations in both the viscosity and thermal conductivity.

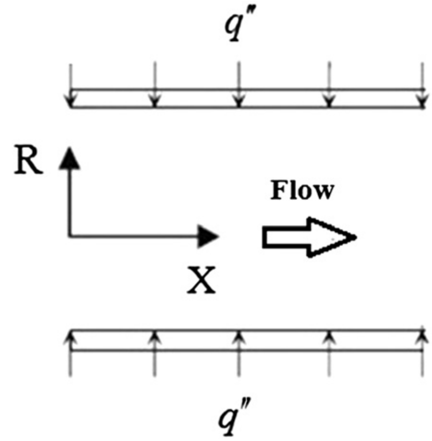

Fig. 1. Isoflux heating applied to a circular channel.

2. Analysis

In this study, hydrodynamically and thermally fully developed, steady state, incompressible and laminar flows of power-law fluids with constant and variable thermophysical properties are analyzed for circular channels under the isoflux thermal boundary condition applied to the tube wall (Fig. 1).

For a power-law fluid, the following shear-stress power-law relationship is valid:

$$\tau = \phi\left|\frac{\partial U}{\partial R}\right|^{n-1}\left(\frac{\partial U}{\partial R}\right) \tag{1}$$

where $\phi\left|\frac{\partial U}{\partial R}\right|^{n-1}$ is viscosity with the consistency factor, ϕ, and the power-law index, n. The governing equations are x-momentum and energy equations, which can be formulated respectively as

$$\frac{1}{R}\frac{\partial}{\partial R}\left(\mu R\frac{\partial U}{\partial R}\right) - \frac{\partial P}{\partial X} = 0 \tag{2}$$

$$\rho c_p U\frac{\partial T}{\partial X} = \frac{1}{R}\frac{\partial}{\partial R}\left(kR\frac{\partial T}{\partial R}\right) + \mu\left(\frac{\partial U}{\partial R}\right)^2 \tag{3}$$

where ρ is the density, P is the pressure, T is the temperature, c_p is the specific heat at constant pressure, k is the thermal conductivity, and U is velocity component in the X direction.

In order to proceed with a solution, viscosity and thermal conductivity must be defined as a function of temperature. Reynolds [44] proposed an exponential model for the temperature-dependence of viscosity as:

$$\mu = \mu_s \exp(-bT) \tag{4}$$

where T is temperature, and μ_s and b are coefficients. Using a truncated Taylor series for $\exp(-bT)$ similar to Hooman and Ejlali [45], viscosity is expressed as:

$$\mu = \mu_s \exp(-bT) = \mu_s\left(1 - \frac{\Delta T}{\mu_s}\frac{d\mu}{dT}\frac{T-\overline{T_w}}{\Delta T}\right) = \mu_s(1-\varepsilon\theta) = \phi(1-\varepsilon\theta)\left|\frac{\partial U}{\partial R}\right|^{n-1} \tag{5}$$

where

$$k = k_s\left(1 + \frac{\Delta T}{\mu_s}\frac{dk}{dT}\frac{T-\overline{T_w}}{\Delta T}\right) = k_s(1+\varepsilon_k\theta) \tag{6}$$

$$\varepsilon = \left.\frac{d\mu}{dT}\right|_{T_s}\frac{\Delta T}{\mu_s} \tag{7}$$

$$\varepsilon_k = \left.\frac{dk}{dT}\right|_{T_s}\frac{\Delta T}{k_s} \tag{8}$$

Here $\frac{T-\overline{T}_w}{\Delta T}$ is the dimensionless temperature, θ. ε_k is defined to be a coefficient of ε, i.e. $\varepsilon_k = \Gamma\varepsilon$, in which Γ can be obtained through computational simulation.

The governing equations for the x-momentum and energy equations can be stated as:

$$\frac{1}{R}\frac{\partial}{\partial R}\left(\mu_s(1-\varepsilon\theta)R\frac{\partial U}{\partial R}\right) - \frac{\partial P}{\partial X} = 0 \tag{9}$$

or

$$\frac{1}{R}\frac{\partial}{\partial R}\left(R\phi(1-\varepsilon\theta)\left|\frac{\partial U}{\partial R}\right|^{n-1}\left(\frac{\partial U}{\partial R}\right)\right) - \frac{\partial P}{\partial X} = 0 \tag{10}$$

$$\rho c_p U\frac{\partial T}{\partial X} = \frac{1}{R}\frac{\partial}{\partial R}\left(k_s(1+\varepsilon_k\theta)R\frac{\partial T}{\partial R}\right) + \left(\phi\left|\frac{\partial U}{\partial R}\right|^{n-1}(1-\varepsilon\theta)\right)\left(\frac{\partial U}{\partial R}\right)^2 \tag{11}$$

To facilitate an analytical solution, the governing equations are non-dimensionalized by using the following non-dimensional parameters and Reynolds number, Re, as:

$$u = \frac{U}{U_m} \quad r = \frac{R}{r_o} \quad x = \frac{X}{r_o} \quad p = \frac{P}{\rho U_m^2} \quad Re = \frac{\rho U_m^{2-n} D^n}{\phi}$$

The dimensionless governing equations are analytically solved to obtain Nusselt number (Nu), as well as the velocity and temperature distributions. The closed form expressions for Nu corresponding to Newtonian liquid flow characteristics can also obtained by setting $n = 1$.

The first step is to derive the velocity distribution. With the introduction of Reynolds number, the non-dimensionalized x-momentum equation becomes:

$$\frac{1}{r}\frac{\partial}{\partial r}\left((1-\varepsilon\theta)r\left(\frac{\partial u}{\partial r}\right)^{n}\right)=\mathrm{Re}\frac{\partial p}{\partial x} \tag{12}$$

The above equation can be solved using the no-slip boundary condition at wall along with the symmetry condition at the center (via setting the axial velocity gradient at the center to zero (i.e., $\partial u/\partial r_{\text{ (at } r\,=\,0)}=0$)).

After implementing the symmetry condition, and using Taylor series with the first order approximation, one can write:

$$\frac{\partial u}{\partial r}=\left(\mathrm{Re}\frac{\partial p}{\partial x}\frac{r}{2}\right)^{\frac{1}{n}}\left(1+\frac{1}{n}\theta\varepsilon\right) \tag{13}$$

For most practical cases, the viscosity variation number is small compared to unity, i.e. $\varepsilon << 1$. This allows for a regular asymptotic expansion assumption (for dependent variables u and θ) in the following form

$$\begin{aligned} u &= u_0+\varepsilon u_1 \\ \theta &= \theta_0+\varepsilon\theta_1 \end{aligned} \tag{14}$$

As a result, Eq. (13) takes the following form:

$$\frac{\partial u_0}{\partial r}+\varepsilon\frac{\partial u_1}{\partial r}=\left(\mathrm{Re}\frac{\partial p}{\partial x}\frac{r}{2}\right)^{\frac{1}{n}}\left(1+\frac{1}{n}\theta_0\varepsilon\right) \tag{15}$$

Splitting the above equation into two following equations

$$\frac{\partial u_0}{\partial r}=\left(\frac{\mathrm{Re}}{2}\frac{\partial p}{\partial x}\right)^{\frac{1}{n}}r^{\frac{1}{n}} \tag{16}$$

$$\varepsilon\frac{\partial u_1}{\partial r}=\varepsilon\left(\frac{\mathrm{Re}}{2}\frac{\partial p}{\partial x}\right)^{\frac{1}{n}}\left(\frac{1}{n}\theta_0\right)r^{\frac{1}{n}} \tag{17}$$

the dimensionless fully developed axial velocity profile, u_0, under the no-slip boundary condition (i.e., $u_{\text{ (at } r\,=\,1)}=0$) is obtained as:

$$u_0=-\frac{1+3n}{1+n}\left(r^{1+\frac{1}{n}}-1\right) \tag{18}$$

In order to find u_1, it is required to proceed with θ_0. For the constant heat flux case, the energy equation containing viscous heating term (viscous dissipation term) should be solved under the no temperature-jump condition, while a constant heat flux is applied at the walls. In the energy equation, the longitudinal temperature gradient, $\partial T/\partial X$, can be obtained with the application of the first law of thermodynamics to an elemental control volume as [46,47]:

$$\dot{m}\,c_p\frac{\partial T}{\partial X}=q''\Lambda+\int\mu\varphi dS \tag{19}$$

For a circular cross-section, it can be written as:

$$\rho U_m R^2 c_p\frac{\partial T}{\partial X}=2q''\left(R+\frac{\phi}{q''}\int_0^{r_0}\left|\frac{\partial U}{\partial R}\right|^{n+1}RdR\right) \tag{20}$$

The above equation can be solved by introducing Brinkman number, defined as $Br=\frac{\phi U_m^{n+1}}{q''D^n}$, and by performing the integral on the right side as:

$$\frac{\partial T}{\partial X}=\frac{q''(A+\varepsilon A')}{\rho U_m R c_p} \tag{21}$$

where the parameter A is expressed as:

$$A=2\left(1+Br\int_0^1\left|\frac{\partial u}{\partial r}\right|^{n+1}rdr\right) \tag{22}$$

or

$$A=2+Br\frac{n}{1+3n}\left|-\frac{1+3n}{n}\right|^{1+n} \tag{23}$$

$$A' = 2\frac{Br}{n}\left|-\frac{1+3n}{n}\right|^{1+n}\int_0^1 |\theta_0| r^{\frac{1+n}{n}} r dr \tag{24}$$

or

$$A' = Br\left|-\frac{1+3n}{n}\right|^{n}\left(\frac{\left(2+8n+Br\left|-\frac{1+3n}{n}\right|^{1+n} n\right)}{(1+3\mathrm{n})(1+5\ \mathrm{n})}\right) \tag{25}$$

Brinkman number, Br, is a dimensionless parameter representing viscous dissipation term. Its positive and negative values refer to wall heating (fluid is being heated) and wall cooling (fluid is being cooled), respectively.

Upon using the dimensionless temperature defined as $\theta = \frac{T-\overline{T}_w}{r_0 q''/k}$, the energy equation takes the following dimensionless form:

$$\begin{aligned} &u_0 A + \varepsilon(u_0 A' + u_1 A) = \frac{1}{r}\frac{\partial}{\partial r}\left(r\frac{\partial\theta_0}{\partial r}\right) + Br\left|\frac{\partial u_0}{\partial r}\right|^{1+n} + \\ &\varepsilon\left[\frac{1}{r}\frac{\partial}{\partial r}\left(r\frac{\partial\theta_1}{\partial r} + \Gamma r\theta_0\frac{\partial\theta_0}{\partial r}\right) + Br(1+n)\left|\frac{\partial u_0}{\partial r}\right|^{n}\frac{\partial u_1}{\partial r} - Br\theta_0\left|\frac{\partial u_0}{\partial r}\right|^{1+n}\right] \end{aligned} \tag{26}$$

or

$$\begin{aligned} &u_0 A + \varepsilon(u_0 A' + u_1 A) = \frac{1}{r}\frac{\partial}{\partial r}\left(r\frac{\partial\theta_0}{\partial r}\right) + Br\left|-\frac{1+3n}{n}\right|^{1+n} r^{\frac{1+n}{n}} + \\ &\varepsilon\left[\frac{1}{r}\frac{\partial}{\partial r}\left(r\frac{\partial\theta_1}{\partial r} + \Gamma r\theta_0\frac{\partial\theta_0}{\partial r}\right) + Br(1+n)\left|-\frac{1+3n}{n}\right|^{n}\left(\frac{\partial u_1}{\partial r}\right) r - Br\theta_0\left|-\frac{1+3n}{n}\right|^{1+n} r^{\frac{1+n}{n}}\right] \end{aligned} \tag{27}$$

Splitting the above equation, the following equations are obtained:

$$u_0 A = \frac{1}{r}\frac{\partial}{\partial r}\left(r\frac{\partial\theta_0}{\partial r}\right) + Br\left|-\frac{1+3n}{n}\right|^{1+n} r^{\frac{1+n}{n}} \tag{28}$$

$$u_0 A' + u_1 A = \left[\frac{1}{r}\frac{\partial}{\partial r}\left(r\frac{\partial\theta_1}{\partial r} + \Gamma r\theta_0\frac{\partial\theta_0}{\partial r}\right) + Br(1+n)\left|-\frac{1+3n}{n}\right|^{n}\left(\frac{\partial u_1}{\partial r}\right) r - Br\theta_0\left|-\frac{1+3n}{n}\right|^{1+n} r^{\frac{1+n}{n}}\right] \tag{29}$$

These equations must be solved subject to the following boundary conditions

$$\begin{aligned} &At\ r = 1 \quad \theta_0 = \theta_1 = 0 \\ &At\ r = 0 \quad \frac{\partial\theta_0}{\partial r} = \frac{\partial\theta_1}{\partial r} = 0 \end{aligned} \tag{30}$$

By substituting u_0, the dimensionless temperature distribution θ_0 is derived as:

$$\theta_0 = \frac{\left(-\frac{(1+3n)A}{1+n} - Br\left|-\frac{1+3n}{n}\right|^{1+n}\right)}{\left(3+\frac{1}{n}\right)^2}\left(r^{3+\frac{1}{n}} - 1\right) + \frac{(1+3n)A}{4(1+n)}\left(r^2 - 1\right) \tag{31}$$

Accordingly, the dimensionless fully developed axial velocity profile, u_1, is obtained as:

$$u_1 = \frac{\left[\begin{aligned} &-2n - 26n^2 - 132n^3 - 324n^4 - 378n^5 - 162n^6 \\ &+\left(1+17n+116n^2+406n^3+765n^4+729n^5+270n^6\right) r^{\frac{1+n}{n}} \\ &-\left(1+15n+92n^2+294n^3+513n^4+459n^5+162n^6\right) r^{\frac{1+3n}{n}} \\ &+\left(2n^2+20n^3+72n^4+108n^5+54n^6\right) r^{\frac{2+4n}{n}} + \\ &Br\left|-\frac{1+3n}{n}\right|^{1+n}\left(\begin{aligned} &\left(n+12n^2+56n^3+126n^4+135n^5+54n^6\right)\left[r^{\frac{1+n}{n}} - r^{\frac{1+3n}{n}}\right] \\ &+\left(n^2+10n^3+36n^4+54n^5+27n^6\right)\left[r^{\frac{2+4n}{n}} - 1\right] \end{aligned}\right) \end{aligned}\right]}{2n(1+n)^2(1+2n)(1+3n)^3} \tag{32}$$

After substituting u_0, u_1, and θ_0 into Eq. (29) and performing several tedious manipulations, a long and complex expression is derived for θ_1 as follows:

$$\theta_1 = C_1\left(r^2 - 1\right) + C_2\left(r^4 - 1\right) + C_3\left(r^{3+\frac{1}{n}} - 1\right) + C_4\left(r^{5+\frac{1}{n}} - 1\right) + C_5\left(r^{6+\frac{2}{n}} - 1\right) \tag{33}$$

where

$$C_1=\frac{\begin{pmatrix}-2+A'+(-12+8A')n+(-18+21A')n^2+18A'n^3+\Gamma\left(1+10n+31n^2+30n^3\right)\\+Br\left|-\frac{1+3n}{n}\right|^{1+n}\left(-3n-9n^2+\Gamma\left(2n+12n^2+16n^3\right)\right)+Br^2\left|-\frac{1+3n}{n}\right|^{2+2n}\left(-n^2+\Gamma\left(n^2+2n^3\right)\right)\end{pmatrix}}{4(1+n)(1+2n)(1+3n)}$$

$$C_2=-\frac{\Gamma\left(1+3n+Br\left|-\frac{1+3n}{n}\right|^{1+n}n\right)^2}{8(1+n)^2}$$

$$C_3=-\frac{\begin{pmatrix}-2n+(-16+2A')n^2+(-30+12A')n^3+18A'n^4+\Gamma\left(2n^2+16n^3+30n^4\right)\\+Br\left|-\frac{1+3n}{n}\right|^{n}\left(1+10n+32n^2+38n^3+15n^4\right)+Br\left|-\frac{1+3n}{n}\right|^{1+n}\left(-3n^2-10n^3+5n^4+\Gamma\left(n^2+10n^3+21n^4\right)\right)\\+Br^2\left|-\frac{1+3n}{n}\right|^{1+2n}\left(n+5n^2+7n^3+3n^4\right)+Br^2\left|-\frac{1+3n}{n}\right|^{2+2n}\left(-n^3+n^4+\Gamma\left(n^3+3n^4\right)\right)\end{pmatrix}}{2(1+n)(1+3n)^3} \tag{34}$$

$$C_4=\frac{\left(1+3n+Br\left|-\frac{1+3n}{n}\right|^{1+n}n\right)\begin{pmatrix}-2n-8n^2-6n^3+\Gamma\left(2n^2+20n^3+50n^4\right)+Br\left|-\frac{1+3n}{n}\right|^{n}\left(1+8n+22n^2+24n^3+9n^4\right)\\+Br\left|-\frac{1+3n}{n}\right|^{1+n}\left(-n^2+2n^3+3n^4+\Gamma\left(n^2+10n^3+25n^4\right)\right)\end{pmatrix}}{2(1+n)^2(1+3n)(1+5n)^2}$$

$$C_5=-\frac{n^2\left(2+Br\left|-\frac{1+3n}{n}\right|^{1+n}\right)}{4(1+n)^2(1+2n)(1+3n)^3}\begin{pmatrix}-n-4n^2-3n^3+\Gamma\left(4n^2+20n^3+24n^4\right)+Br\left|-\frac{1+3n}{n}\right|^{n}\left(1+7n+17n^2+17n^3+6n^4\right)\\+Br\left|-\frac{1+3n}{n}\right|^{1+n}\left(2n^3+2n^4+\Gamma\left(2n^2+10n^3+12n^4\right)\right)\end{pmatrix}$$

Determined velocities (u_0, u_1) and temperatures (θ_0 and θ_1) are utilized to find the dimensionless bulk or mean temperature given as:

$$\theta_m=\frac{\int u\theta dS}{\int udS}=2\int_0^1[u_0\theta_0+\varepsilon(u_0\theta_1+u_1\theta_0)]rdr \tag{35}$$

Nusselt number is defined as $Nu=\frac{Dq''}{k(\overline{T}_w-T_m)}$ and can be also written in terms of the dimensionless temperature as:

$$Nu=\frac{-2}{\theta_m} \tag{36}$$

In the case of constant properties, Nusselt number can be expressed in the following form as:

$$Nu=\frac{8(1+3n)(1+5n)}{1+12n+31n^2+Br(1+3n)(1+5n)\left|-\frac{1+3n}{n}\right|^{n}} \tag{37}$$

To the authors' best knowledge, there are no other studies in the literature, in which the viscous dissipation term is present. However, the results of Eq. (37) are in excellent agreement with those of Barkhordari and Etemad [48] in the absence of viscous heating and with those of Hooman [46] in the presence of viscous heating and $n = 1$.

For the variable property case, it is not possible to give an explicit expression for Nusselt number. Therefore, a numerical analysis is needed. In order to have a better design and improvement in thermo-fluidic systems, the second law analysis constitutes an important part of analysis. In this point of view, the entropy generation, which is dependent on irreversibilities in fluid friction and heat transfer due to existence of gradients in velocity and temperature, plays a significant role in such systems. Therefore, minimization of entropy generation through reducing the irreversibilities would be a desirable goal for thermo-fluid researchers to augment the system efficiency. In this regard, the second law analysis is investigated in the current study to provide some insight on how the governing parameters affect the entropy generation rate. The volumetric rate of entropy generation can be expressed as [49]:

$$\dot{S}=\frac{k}{T^2}(\nabla T.\nabla T)+\frac{\mu\varphi}{T} \tag{38}$$

where the first and second terms on the right side are (volumetric) Heat Transfer Irreversibility and Fluid Friction Irreversibility, respectively.

For the case of non-Newtonian fluids, entropy generation rate is derived as:

$$\dot{S}=\frac{k_s(1+\varepsilon_k\theta)}{T_i^2}\left(\left(\frac{\partial T}{\partial X}\right)^2+\left(\frac{\partial T}{\partial R}\right)^2\right)+\frac{\phi}{T_i}(1-\varepsilon\theta)\left|\frac{\partial U}{\partial R}\right|^{n-1}\left(\frac{\partial U}{\partial R}\right)^2 \tag{39}$$

In non-dimensional form, it can be expressed as:

$$N_s = \dot{S}\frac{{r_0}^2}{k_s\Omega^2} = (1+\varepsilon_k\theta)\left(\left(\frac{A+\varepsilon A'}{Pe}\right)^2 + \left(\frac{\partial\theta_0}{\partial r}+\varepsilon\frac{\partial\theta_1}{\partial r}\right)^2\right) + \frac{Br}{\Omega}(1-\varepsilon\theta)\left|\frac{\partial u_0}{\partial r}+\varepsilon\frac{\partial u_1}{\partial r}\right|^{n+1} \tag{40}$$

After simplifications and rearrangements, and neglecting higher-order terms o(ε^2), it becomes:

$$\begin{aligned} N_s = \dot{S}\frac{{r_0}^2}{k\Omega^2} = &\left(\frac{A}{Pe}\right)^2 + \left(\frac{\partial\theta_0}{\partial r}\right)^2 + \frac{Br}{\Omega}\left|\frac{\partial u_0}{\partial r}\right|^{n+1} + \\ &\varepsilon\left(\Gamma\theta_0\left(\frac{A}{Pe}\right)^2 + \Gamma\theta_0\left(\frac{\partial\theta_0}{\partial r}\right)^2 + \frac{2AA'}{Pe^2} + 2\frac{\partial\theta_0}{\partial r}\frac{\partial\theta_1}{\partial r} - \frac{Br}{\Omega}\theta_0\left|\frac{\partial u_0}{\partial r}\right|^{n+1} + \frac{Br}{\Omega}(1+n)\frac{\partial u_1}{\partial r}\left|\frac{\partial u_0}{\partial r}\right|^{n}\right) \end{aligned} \tag{41}$$

where $\Omega = q^{''} r_0/T_i k$ and Pe is Peclet number. The temperature and velocity gradients are as follows:

$$\begin{aligned} \frac{\partial u_0}{\partial r} &= -\frac{1+3n}{n} r^{\frac{1}{n}} \\ \frac{\partial u_1}{\partial r} &= \frac{\left[\begin{array}{l} \left(\frac{1+n}{n}\right)\left(1+17n+116n^2+406n^3+765n^4+729n^5+270n^6\right)r^{\frac{1}{n}} \\ -\left(\frac{1+3n}{n}\right)\left(1+15n+92n^2+294n^3+513n^4+459n^5+162n^6\right)r^{\frac{1+2n}{n}} \\ +\left(\frac{2+4n}{n}\right)\left(2n^2+20n^3+72n^4+108n^5+54n^6\right)r^{\frac{2+3n}{n}} + \\ Br\left|-\frac{1+3n}{n}\right|^{1+n}\left(\begin{array}{l} \left(n+12n^2+56n^3+126n^4+135n^5+54n^6\right)\left[\left(\frac{1+n}{n}\right)r^{\frac{1}{n}} - \left(\frac{1+3n}{n}\right)r^{\frac{1+2n}{n}}\right] \\ +\left(n^2+10n^3+36n^4+54n^5+27n^6\right)\left[\left(\frac{2+4n}{n}\right)r^{\frac{2+3n}{n}}\right] \end{array}\right) \end{array}\right]}{2n(1+n)^2(1+2n)(1+3n)^3} \\ \frac{\partial\theta_0}{\partial r} &= \frac{\left(-\frac{(1+3n)A}{1+n} - Br\left|-\frac{1+3n}{n}\right|^{1+n}\right)}{3+\frac{1}{n}} r^{2+\frac{1}{n}} + \frac{(1+3n)A}{2(1+n)} r \\ \frac{\partial\theta_1}{\partial r} &= 2C_1 r + 4C_2 r^3 + C_3\frac{1+3n}{n} r^{\frac{1+2n}{n}} + C_4\frac{1+5n}{n} r^{\frac{1+4n}{n}} + C_5\frac{2+6n}{n} r^{\frac{2+5n}{n}} \end{aligned} \tag{42}$$

The main aim of second law analysis is to find parameters minimizing global entropy generation rate, denoted by $<N_s>$, which is related to the whole dissipations generated by irreversibilities in the channel. Therefore, it is required to integrate N_s across the cross-sectional area occupied by the fluid through $<N_s> = \int N_s dS/S$, and can be written as:

$$<N_s> = \int_0^1 2N_s r dr \tag{43}$$

Again, it is needed to perform numerical analysis to obtain the global entropy generation.

3. Results and discussion

As pointed out earlier, viscosity and thermal conductivity vary with temperature so that a rise in temperature leads to a decrease in viscosity and an increase in thermal conductivity. This section includes the effect of variable properties and viscous dissipation on the entropy generation rate and heat transfer characteristics of hydrodynamically and thermally fully developed non-Newtonian flows in tubes at isoflux boundary condition while assuming a power-law fluid model.

Shear-thinning (or pseudoplastic) fluids having power-law index in the range $0 < n < 1$ behaves in such a way that their viscosity decreases with shear rate, while this behavior is otherwise for shear-thickening (or dilatants) fluids having power-law index larger than unity ($n > 1$).

In order to verify the analytical results in the case of variable property, a numerical simulation was carried out by employing ANSYS FLUENT 14.0 software that compares the numerical and analytical results of fully developed dimensionless velocity profile. The temperature-dependent viscosity equation based on the experimental data expression given in Ref. [50] was implemented in the software through a User-Defined Function (UDS) as following

$$\mu(T) = 0.00002414 \times 10^{\frac{247.8}{T-140}} \tag{44}$$

where T has units of Kelvin, and μ has units of N·s/m^2.

Fig. 2 demonstrates the comparison between numerical (at $Re = 10$) and analytical solutions, which shows a good agreement. It is notable that analytical results correspond to $\varepsilon = 0.064$, which was acquired by Eq. (7) from the numerical analysis. The value of Γ can be also obtained by the numerical simulation, which is dependent on the applied heat flux. For example, for water as a working fluid under heat flux of 50,000 W/m^2 the value of Γ is 0.076. For the sake of simplicity and consistency, throughout this study it is taken to be $\Gamma = 0.2$.

Fig. 3 illustrates the dimensionless velocity distribution at various power-law indices, n, for both constant and variable properties at $Br = 0.01$. As seen, regardless of the property, the core velocity of the flow moves faster when the power-law index increases, while its velocity near the walls takes smaller values to keep the flow rate constant.

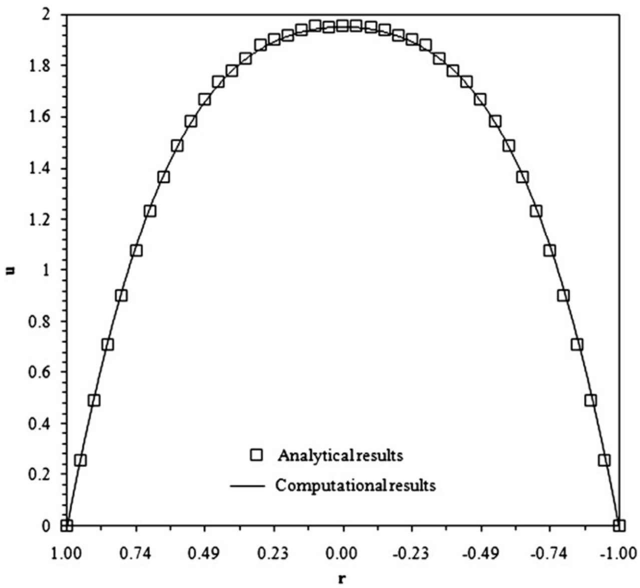

Fig. 2. Comparison between numerical results of temperature-dependent viscosity of water given in Ref. [50] and analytical result corresponding to $\varepsilon = 0.064$.

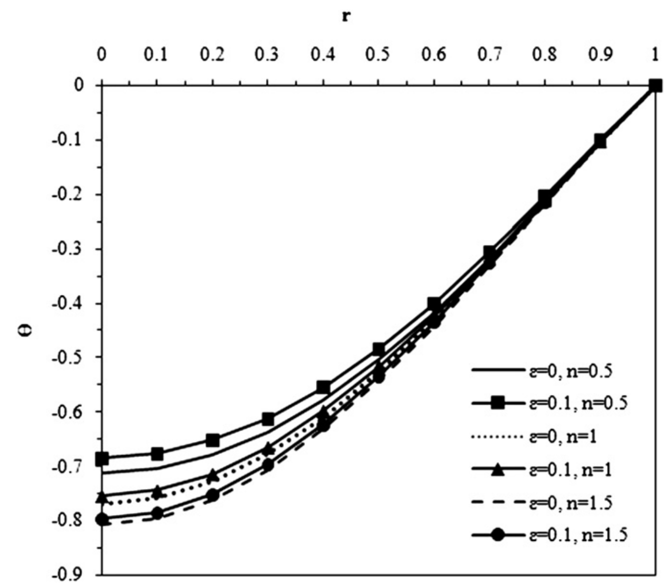

Fig. 4. Dimensionless fully developed temperature profiles for different values of n for constant and variable property cases at $Br = 0.01$.

Generally, the parabolic profile regarding to Newtonian fluid ($n = 1$) deforms to a more uniform profile compared to shear-thinning fluids and to a more non-uniform profile compared to shear-thickening fluids. Furthermore, the consideration of temperature-dependent properties slightly decreases the velocity values at the core region. This trend is due to the decreasing viscosity with temperature hence giving rise to lower pressure drop and accordingly lower velocities.

Fig. 4 shows the dimensionless temperature distribution of the flow for different values of n in the cases of $\varepsilon = 0$ and $\varepsilon = 0.1$ at $Br = 0.01$. Similar to velocity profiles, the temperature develops in the core region for increasing power-law index. It was also observed that a slight increase in the fluid temperature exists for all types of the fluids, but more effectively for shear-thinning fluid, at the core region by taking the variable properties. The temperature increment may be ascribed to the enhancing effect of thermal conductivity of the fluid owing to the temperature variation.

Fig. 5 shows the variation of Nusselt number as a function of power-law index for different Brinkman numbers in the case of both constant ($\varepsilon = 0$) and variable property ($\varepsilon = 0.1$) cases. It can be observed that Nusselt number decreases with both the power-law index and Brinkman number, regardless of the property. However, this decreasing trend is more significantly seen at higher Brinkman numbers, which is because Brinkman number appearing as a coefficient in the viscous dissipation term leads to viscous heating, and accordingly, it gives rise to an increase in the mean temperature of the fluid through the internal heating and ultimately to the decrease in Nusselt number. It is also noticeable that the effect of Brinkman number on *Nu* becomes more significant for shear-thickening fluids, which is attributed to higher mean temperatures. In the case of the variable thermophysical property

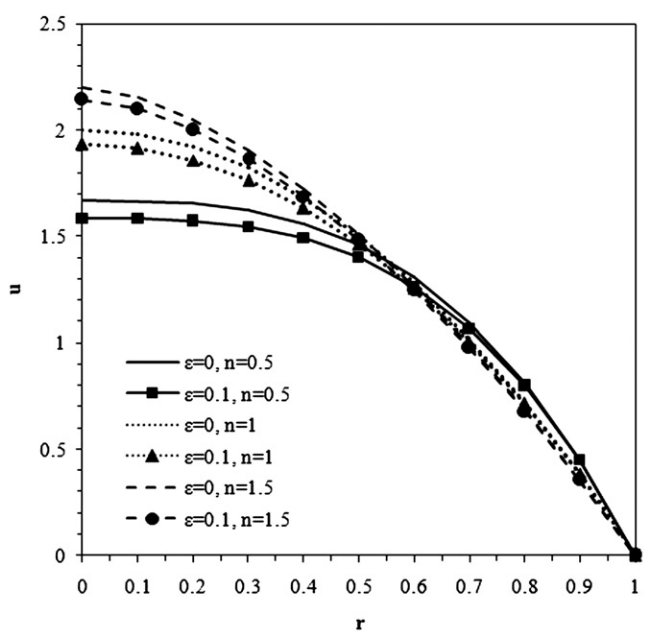

Fig. 3. Dimensionless fully developed velocity profiles for different values of n for constant and variable property case at $Br = 0.01$.

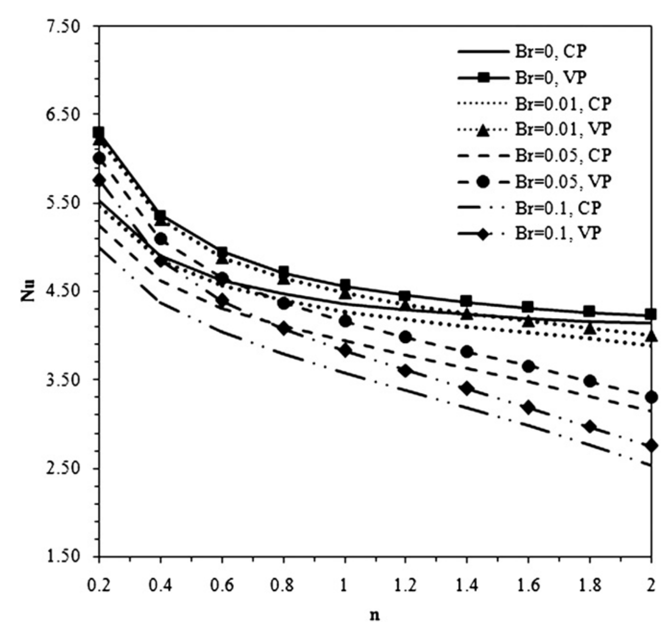

Fig. 5. Nusselt number as a function of n for different values of Br at the constant (at $\varepsilon = 0$) and variable property (at $\varepsilon = 0.1$) cases.

case, the values of Nusselt number are larger compared to the constant property case. However, the effect of property variation on the heat transfer rate becomes less significant when the power-law index goes higher in the shear-thickening fluid range for low *Br*. For example, for $n = 2$ and $Br = 0.1$, the change in Nusselt number is about 8% due to the consideration of the variable properties. For shear-thinning fluid, the values of Nusselt number are more underestimated by neglecting the temperature-variation effect. For instance, at $n = 0.2$ and $Br = 0.1$, the deviation becomes more and reaches about 13%. Indeed, the viscosity decreases with temperature, which causes an increase in Reynolds number and consequently has a positive effect on heat transfer and Nusselt number. On the other hand, the thermal conductivity has an increasing trend with temperature, and has a negative effect on Nusselt number ($Nu = hd/k$). As a result, there is an interplay between viscosity and thermal conductivity effects, where the viscosity dominates giving rise to an increase in Nusselt number.

The effect of property variation (perturbation parameter) on the heat transfer rate for different n and $Br = 0.01$ is displayed in Fig. 6. As mentioned earlier, heat transfer is reduced when the power-law index is increased. It can be seen that heat transfer rate (Nusselt number value) increases for the variable thermophysical property case and with ε at which the deviation from constant properties might reach about 32.6%. However, the effect of property diminishes as the power-law index becomes larger, in particular for shear-thickening fluids, where a relatively smaller change is observed for $n = 2$.

Table 1 presents the global entropy generation rate, $<Ns>$, versus power-law index at $\varepsilon = 0.1$ and various Brinkman numbers in absence of axial heat conduction term corresponding to $Pe \rightarrow \infty$. As can be seen from the table, except for $Br = 0.01$ (which will be depicted in the next figure), the global entropy generation rate increases with power-law index for both constant property and variable property cases particularly for higher *Br*. Since lower value of entropy generation would imply a better working performance, the fluidic system with smaller *Br* (or smaller viscous heating) is desirable, which leads to a more efficient convective heat transfer as well. Furthermore, lower values of the global entropy generation rate are obtained for lower n (i.e. shear-thining fluids), which is due to smaller velocity and temperature gradients at the walls, where the entropy generation is more pronounced. Entropy generation rate reaches its maximum and minimum values at the wall and center, respectively, where the maximum and minimum (zero for this case) velocity and temperature gradients are present. From this table, it can be also understood that the property variation with temperature causes a decrease in $<Ns>$ for all values of *Br*. Indeed, the perturbed

Table 1
The values of global entropy generation rate at $\Omega = 0.1$, $Pe = \infty$ for different *Br* and n.

	Constant property				Variable property ($\varepsilon = 0.1$)			
	Br				*Br*			
	0	0.01	0.05	0.1	0	0.01	0.05	0.1
n								
0.2	0.725	0.526	0.986	2.373	0.636	0.45	0.954	2.273
0.4	0.815	0.806	1.906	3.767	0.745	0.739	1.82	3.61
0.6	0.864	1.15	2.982	5.5	0.808	1.085	2.861	5.286
0.8	0.895	1.49	4.09	7.41	0.849	1.426	3.945	7.148
1	0.917	1.757	5.13	9.37	0.877	1.696	4.971	9.07
1.2	0.932	1.889	6.031	11.293	0.898	1.833	5.871	10.974
1.4	0.944	1.837	6.789	13.181	0.914	1.791	6.643	12.874
1.6	0.954	1.591	7.537	15.214	0.927	1.561	7.422	14.96
1.8	0.961	1.267	8.619	17.847	0.938	1.259	8.545	17.679
2	0.968	1.355	10.551	21.83	0.947	1.361	10.497	21.724

term contributes to the reduction of the global entropy generation by decreasing the irreversibility caused by viscous heating through the velocity gradient portion.

The variation in the global entropy generation as a function of power-law index at $Br = 0.01$, $\Omega = 0.1$, and different values of ε is depicted in Fig. 7. The global entropy generation increases with n to its maximum value around $n = 1.2$ and then starts decreasing until $n = 1.8$. An unexpected trend after this point is seen where the value of $<Ns>$ again increases with n. Additionally, one can observe that an increment in ε leads to a decrease in $<Ns>$, except for very high values of n which are insensitive to property variation.

Table 2 exhibits the values of the global entropy generation rate, $<N_s>$, as a function of power-law index at $Br = 0.01$, $\Omega = 0.1$ and different values of Peclet number, *Pe*, which represents the axial heat conduction effect on the entropy generation. It is worthwhile noting that Peclet number does not play any role in the heat transfer analysis of fully developed flows due to the constant axial temperature gradient. The results in the table also reveal that the increase in *Pe* (axial heat conduction portion) generally leads a decrease in the values of $<N_s>$. For very low values of *Pe* (here $Pe = 0.1$) the global entropy generation rate increases with n, which means that shear-thickening fluids generate more irreversibilities compared to shear-thinning ones. However, for other *Pe* values, the trend is very similar to that of Fig. 7. Furthermore, the values of $<N_s>$ decrease with inclusion of temperature-dependent properties, except for very high values of n. This means that irreversibilities due to heat transfer and fluid friction are lowered by inserting

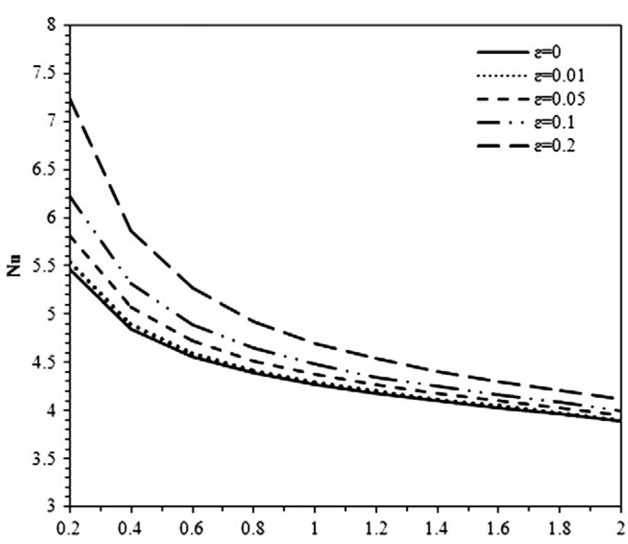

Fig. 6. Nusselt number as a function of n for different values of ε at $Br = 0.01$.

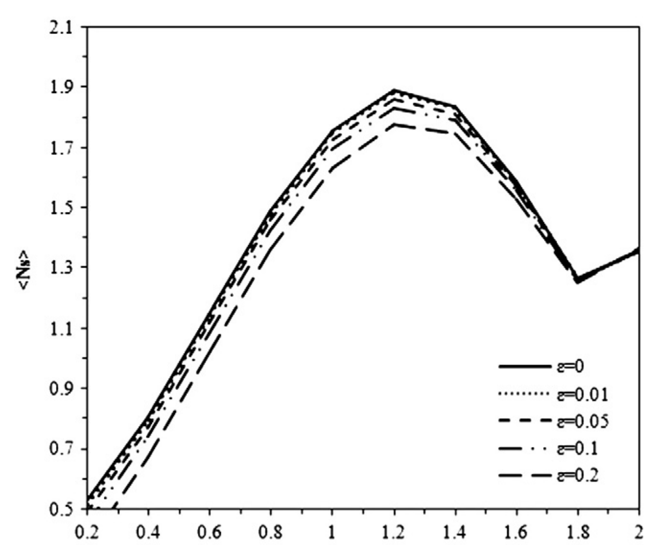

Fig. 7. Global entropy generation rate as a function of n for different values of ε at $\Omega = 0.1$and $Br = 0.01$.

Table 2
The values of global entropy generation rate at $\Omega = 0.1$, $Br = 0.01$ for different n and ε.

n	$\varepsilon = 0$, $Pe = 0.1$	$\varepsilon = 0$, $Pe = 10$	$\varepsilon = 0$, $Pe = 100$	$\varepsilon = 0.1$, $Pe = 0.1$	$\varepsilon = 0.1$, $Pe = 10$	$\varepsilon = 0.1$, $Pe = 100$
0.2	412.713	0.565	0.526	410.834	0.489	0.451
0.4	416.69	0.843	0.806	414.599	0.776	0.739
0.6	421.46	1.188	1.15	419.259	1.123	1.086
0.8	427.304	1.531	1.49	425.041	1.467	1.426
1	434.397	1.8	1.758	432.098	1.739	1.696
1.2	442.923	1.931	1.89	440.607	1.875	1.834
1.4	453.199	1.872	1.838	450.881	1.826	1.792
1.6	465.82	1.608	1.591	463.51	1.577	1.561
1.8	481.799	1.248	1.267	479.5	1.239	1.259
2	502.647	1.305	1.355	500.356	1.311	1.36

variable properties. Therefore, the results suggest that if thermophysical properties are not considered as variable there will be an overestimation of $\langle N_s \rangle$.

4. Conclusion

Convective heat transfer analysis and second law analysis were performed to reveal the effects of variable thermophysical properties, namely viscosity and thermal conductivity, power-law index and viscous dissipation on heat transfer characteristics of hydrodynamically and thermally fully developed power-law fluid flows in tubes under uniform heat flux thermal boundary conditions. Aside from deriving the velocity and temperature distributions, Nusselt number and entropy generation rate have been examined along with their trends with key parameters being power-law index, Brinkman number, and property variation. Major conclusions of this study are as follows:

- Nusselt number decreases with increasing both power-law index and Brinkman number, regardless of the change in thermophysical properties with temperature.
- The variation in thermophysical properties with temperature has an increasing effect on Nusselt number compared to the constant property case.
- Except for few cases, the rate of global entropy generation, $\langle N_s \rangle$, increases with power-law index, Brinkman number, whereas thermophysical property variation effect causes a decrease in $\langle N_s \rangle$.

Acknowledgments

This work was supported by TUBA (Turkish Academy of Sciences) Outstanding Young Investigator Support Program (TUBA GEBIP 2011/13). Graduate student support from Faculty of Natural Sciences and Engineering of Sabancı University and Sabancı University Nanotechnology Research and Applications Center (SUNUM) is also gratefully appreciated.

References

[1] A. Acrivos, M.J. Shah, E.E. Petersen, Momentum and heat transfer in laminar boundary-layer flows of non-Newtonian fluids past external surfaces, AICHE J. 6 (1960) 312–317.
[2] M. Akçay, M.A. Yükselen, Drag reduction of a non-Newtonian fluid by fluid injection on a moving wall, Arch. Appl. Mech. 69 (1999) 215–225.
[3] A. Pinarbasi, M. Imal, Viscous heating effects on the linear stability of Poiseuille flow of an inelastic fluid, J. Non-Newtonian Fluid Mech. 127 (2005) 67–71.
[4] C.H. Chen, Effect of viscous dissipation on heat transfer in a non-Newtonian liquid film over an unsteady stretching sheet, J. Non-Newtonian Fluid Mech. 135 (2005) 128–135.
[5] S.S. Pawar, V.K. Sunnapwar, Experimental studies on heat transfer to Newtonian and non-Newtonian fluids in helical coils with laminar and turbulent flow, Exp. Thermal Fluid Sci. 44 (2013) 792–804.
[6] S.D. Joshi, A.E. Bergles, Experimental study of laminar heat transfer to in-tube flow of non-Newtonian fluids, J. Heat Transf. 102 (1980) 397–401.
[7] S.Gh. Etemad, Viscous non-Newtonian forced convection heat transfer in semi-circular and equilateral triangular ducts: an experimental study, Int. Commun. Heat Mass Transfer 24 (1997) 609–620.
[8] I. Filkova, A. Lawal, B. Koziskova, A.S. Mujumdar, Heat transfer to a power-law fluid in tube flow: numerical and experimental studies, J. Food Eng. 6 (1987) 143–151.
[9] D. Béreiziat, R. Devienne, Experimental characterization of Newtonian and non-Newtonian fluid flows in corrugated channels, Int. J. Eng. Sci. 37 (1999) 1461–1479.
[10] M. Gradeck, B.F.Z. Fagla, C. Baravian, M. Lebouché, Experimental thermomechanic study of Newtonian and non-Newtonian suspension flows, Int. J. Heat Mass Transfer 16 (2005) 3469–3477.
[11] H. Ragueb, K. Mansouri, A numerical study of viscous dissipation effect on non-Newtonian fluid flow inside elliptical duct, Energy Convers. Manag. 68 (2013) 124–132.
[12] A. Filali, L. Khezzar, D. Siginer, Z. Nemouchi, Graetz problem with non-linear viscoelastic fluids in non-circular tubes, Int. J. Therm. Sci. 61 (2012) 50–60.
[13] P.S.B. Zdanski, M. Vaz, A.P.C. Dias, Forced convection heat transfer of polymer melt flow inside channels with contraction/expansion sections, Int. Commun. Heat Mass Transfer 38 (2011) 1335–1339.
[14] S. Poncet, S. Haddadi, S. Viazzo, Numerical modeling of fluid flow and heat transfer in a narrow Taylor–Couette–Poiseuille system, Int. J. Heat Fluid Flow 32 (2011) 128–144.
[15] M. Capobianchi, D. Wagner, Heat transfer in laminar flows of extended modified power law fluids in rectangular ducts, Int. J. Heat Mass Transf. 53 (2010) 558–563.
[16] M. Habibi Matin, W.A. Khan, Laminar natural convection of non-Newtonian power-law fluids between concentric circular cylinders, Int. Commun. Heat Mass Transfer 43 (2013) 112–121.
[17] R.Y. Jumah, A.S. Mujumdar, Free convection heat and mass transfer of non-Newtonian power law fluids with yield stress from a vertical flat plate in saturated porous media, Int. Commun. Heat Mass Transfer 27 (2000) 485–494.
[18] M. Lamsaadi, M. Naïmi, M. Hasnaoui, Natural convection of non-Newtonian power law fluids in a shallow horizontal rectangular cavity uniformly heated from below, Heat Mass Transf. 41 (2005) 239–249.
[19] A. Guha, K. Pradhan, Natural convection of non-Newtonian power-law fluids on a horizontal plate, Int. J. Heat Mass Transf. 70 (2014) 930–938.
[20] N.T.M. Eldabe, M.F. El-Sayed, A.Y. Ghaly, H.M. Sayed, Mixed convective heat and mass transfer in a non-Newtonian fluid at a peristaltic surface with temperature-dependent viscosity, Arch. Appl. Mech. 78 (2008) 599–624.
[21] T.Y. Wang, Mixed convection from a vertical plate to non-Newtonian fluids with uniform surface heat flux, Int. Commun. Heat Mass Transfer 22 (1995) 369–380.
[22] M. Amoura, N. Zeraibi, A. Smati, M. Gareche, Finite element study of mixed convection for non-Newtonian fluid between two coaxial rotating cylinders, Int. Commun. Heat Mass Transfer 33 (2006) 780–789.
[23] C.C. Wang, C.K. Chen, Mixed convection boundary layer flow of non-Newtonian fluids along vertical wavy plates, Int. J. Heat Fluid Flow 23 (2002) 831–839.
[24] C.H. Chen, Effects of magnetic field and suction/injection on convection heat transfer of non-Newtonian power-law fluids past a power-law stretched sheet with surface heat flux, Int. J. Therm. Sci. 47 (2008) 954–961.
[25] E.M. Abo-Eldahab, A.M. Salem, MHD Flow and heat transfer of non-Newtonian power-law fluid with diffusion and chemical reaction on a moving cylinder, Heat Mass Transf. 41 (2005) 703–708.
[26] K.V. Prasad, D. Pal, V. Umesh, N.S. Prasanna Rao, The effect of variable viscosity on MHD viscoelastic fluid flow and heat transfer over a stretching sheet, Commun. Nonlinear Sci. Numer. Simul. 15 (2010) 331–344.
[27] A. Babaie, M.H. Saidi, A. Sadeghi, Heat transfer characteristics of mixed electroosmotic and pressure driven flow of power-law fluids in a slit microchannel, Int. J. Therm. Sci. 53 (2012) 71–79.
[28] C. Zhao, C. Yang, Joule heating induced heat transfer for electroosmotic flow of power-law fluids in a microcapillary, Int. J. Heat Mass Transfer 55 (2012) 2044–2051.
[29] S. Sánchez, J. Arcos, O. Bautista, F. Méndez, Joule heating effect on a purely electroosmotic flow of non-Newtonian fluids in a slit microchannel, J. Non-Newtonian Fluid Mech. 192 (2013) 1–9.
[30] R. Chiba, M. Izumi, Y. sugano, An analytical solution to non-axisymmetric heat transfer with viscous dissipation for non-Newtonian fluids in laminar forced flow, Arch. Appl. Mech. 78 (2008) 61–74.
[31] F.T. Pinho, P.M. Coelho, Fully-developed heat transfer in annuli for viscoelastic fluids with viscous dissipation, J. Non-Newtonian Fluid Mech. 138 (2006) 7–21.
[32] R.M. Manglik, J. Ding, Laminar flow heat transfer to viscous powerlaw fluids in double-sine ducts, Int. J. Heat Mass Transf. 40 (1997) 1379–1390.
[33] N. Thayalan, Y.M. Hung, Momentum integral method for forced convection in thermal nonequilibrium power-law fluid-saturated porous media, Chem. Eng. Commun. 200 (2013) 269–288.
[34] C.H. Chen, Electro-osmotic heat transfer of non-Newtonian fluid flow in microchannels, J. Heat Transf. Trans. ASME 133 (2011) 071705.
[35] A. Jabari Moghadam, Electrokinetic-driven flow and heat transfer of a non-Newtonian fluid in a circular microchannel, J. Heat Transf. 135 (2013) 021705.
[36] A. Sadeghi, M.H. Saidi, A.A. Mozafari, Heat transfer due to electroosmotic flow of viscoelastic fluids in a slit microchannel, Int. J. Heat Mass Transfer 54 (2011) 4069–4077.
[37] C.P. Tso, J. Sheela-Francisca, Y.M. Hung, Viscous dissipation effects of power-law fluid flow within parallel plates with constant heat fluxes, J. Non-Newtonian Fluid Mech. 165 (2010) 625–630.
[38] S. Mahmud, F.R. Fraser, Asymptotic Nusselt and entropy generation numbers for non-Newtonian fluid flow, Heat Mass Transf. 41 (2005) 999–1003.

[39] M. Shojaeian, A. Koşar, Convective heat transfer and entropy generation analysis on Newtonian and non-Newtonian fluid flows between parallel-plates under slip boundary conditions, Int. J. Heat Mass Transfer 70 (2014) 664–673.
[40] L.C. Zheng, X.X. Zhang, L.X. Ma, Fully developed convective heat transfer of power law fluids in a circular tube, Chin. Phys. Lett. 25 (2008) 195–197.
[41] M.E. Sayed-Ahmed, The effect of variable properties on the helical flow and heat transfer of power law fluids, Acta Mech. 181 (2006) 185–197.
[42] J.M. Nóbrega, F.T. Pinho, P.J. Oliveira, O.S. Carneiro, Accounting for temperature-dependent properties in viscoelastic duct flows, Int. J. Heat Mass Transfer 47 (2004) 1141–1158.
[43] A. Molaei Dehkordi, M. Memari, Transient and steady-state forced convection to power-law fluids in the thermal entrance region of circular ducts: effects of viscous dissipation, variable viscosity, and axial conduction, Energy Convers. Manag. 51 (2010) 1065–1074.
[44] O. Reynolds, On the theory of lubrication and its application to beauchamp tower's experiments, Philos. Trans. R. Soc. Lond. 177 (1886) 157–234.
[45] K. Hooman, A. Ejlali, Effects of viscous heating, fluid property variation, velocity slip, and temperature jump on convection through parallel plate and circular microchannels, Int. Commun. Heat Mass Transfer 37 (2010) 34–38.
[46] K. Hooman, Entropy generation for microscale forced convection: effects of different thermal boundary conditions, velocity slip, temperature jump, viscous dissipation, and duct geometry, Int. Commun. Heat Mass Transfer 34 (2007) 945–957.
[47] M. Shojaeian, S.M.N. Shojaee, Viscous dissipation effect on heat transfer characteristics of mixed electromagnetic/pressure driven liquid flows inside micropumps, Korean J. Chem. Eng. 30 (2013) 823–830.
[48] M. Barkhordari, S.Gh. Etemad, Numerical study of slip flow heat transfer of non-Newtonian fluids in circular microchannels, Int. J. Heat Fluid Flow 28 (2007) 1027–1033.
[49] A. Bejan, Entropy Generation Through Heat and Fluid Flow, Wiley, New York, 1982.
[50] T. Al-Shemmeri, Engineering Fluid Mechnanics, Ventus Publishing ApS, 2012, ISBN 978-87-403-0114-4. 17–18.